Received: 31 March 2022 | Accepted: 30 May 2022

DOI: 10.1002/bab.2372

ORIGINAL ARTICLE

WILEY

Immuno-probed multiwalled carbon nanotube surface for abdominal aortic aneurysm biomarker analysis

Xuekai Zhao[1] | **Subash C.B. Gopinath**[2,3,4] | **Weichao Zhao**[5]

[1]Department of Cardiovascular Surgery, Zibo Central Hospital, Zibo, Shandong Province, China

[2]Faculty of Chemical Engineering Technology, Universiti Malaysia Perlis (UniMAP), Arau, Perlis, 02600, Malaysia

[3]Institute of Nano Electronic Engineering, Universiti Malaysia Perlis (UniMAP), Kangar, Perlis, 01000, Malaysia

[4]Centre of Excellence for Nanobiotechnology and Nanomedicine (CoExNano), Faculty of Applied Sciences, AIMST University, Semeling, Kedah, Malaysia

[5]Department of Cardiovascular Surgery, The Fourth Hospital of Hebei Medical, University, Shijiazhuang, Hebei Province, China

Correspondence
Weichao Zhao, Department of Cardiovascular Surgery, The Fourth Hospital of Hebei Medical, University, Shijiazhuang, Hebei Province, 051411, China.
Email: Weichao777888@sina.com

Abstract

Abdominal aortic aneurysm (AAA), a medical complication, occurs when the aortic area becomes swollen and very large. It is mandatory to identify AAA to avoid the breakdown of aneurysms. C-reactive protein (CRP) has been recognized as one of the biomarkers for identifying AAA due to the possibility of CRP produced in vascular tissue, which contributes to the formation of an aneurysm, and it is elevated in patients with a ruptured AAA. This research work was designed to develop an immunosensor on a multiwalled carbon nanotube (MWCNT)-modified surface to quantify the CRP level. Anti-CRP specificity was constructed on the MWCNT surface through a silane linker to interact with CRP. The detection limit of CRP was calculated as 100 pM with an R^2 (determination coefficient) value of 0.9855 ($y = 2.3446x - 1.9922$) on a linear regression graph. The dose-dependent linear pattern was registered from 200 to 3000 pM and attained the saturation level during binding at 3000 pM. Furthermore, serum-spiked CRP showed a clear increase in the current response, proving the specific recognition of CRP in biological samples. This designed biosensor identifies CRP at a lower level and can help diagnose AAA.

KEYWORDS

aortic swelling, biomarker, biosensor, C-reactive protein, immunoassay

1 | INTRODUCTION

The aorta is a larger blood vessel that helps to carry out oxygenated blood from the heart to the entire body.[1–3] An abdominal aortic aneurysm (AAA) is a bulging and stretched area in the aorta.[4] The bulging area weakens the aorta, and it may burst when ruptures occur, which causes life-threatening bleeding. An aortic diameter of less than 3 cm is considered normal, and an aortic diameter of >3 cm is considered a serious issue.[5] Therefore, identifying AAAs and their sizes is mandatory to avoid rupturing of the aneurysm. Ultrasound has been commonly conducted to identify AAAs and their size. Blood-based biomarkers help diagnose AAAs and for follow-up treatment after AAA surgery. Various blood-based biomarkers have been effectively used to identify different diseases at the earlier stages.[6–9] Circulating serum biomarkers are predominantly involved in the progression of an AAA and its size changes. Circulating inflammatory cytokines

Abbreviations: AAA, Abdominal aortic aneurysm; CRP, C-reactive protein; MWCNT, Multiwalled carbon nanotube; cm, Centimeter; CNT, Carbon nanotubes; APTMS, (3-aminopropyl)trimethoxysilane; GLU, Glutaraldehyde; μm, Micrometer; RCA, Radio corporation of America; IDE, Interdigitated electrode; KOH, Potassium hydroxide; nM, Nanomolar; h, Hour; pM, Picomolar; PBS, Phosphate buffered saline; M, Molar.

were found to be elevated in AAA patients, and higher expression of proinflammatory cytokines was identified in the aneurysmal tissue. Furthermore, the serum concentration of various cytokines is highly associated with the diameter of the aneurysm. In addition, insulin-like growth hormone levels play a vital role in aneurysm growth. Similar to other biomarkers, researchers found that C-reactive protein (CRP) can be a suitable marker for AAA diagnosis. CRP is produced by the liver and is one of the highly expressed proteins during the inflammatory process. Researchers have found that CRP levels are higher in patients with ruptured and symptomatic AAA.[10] Furthermore, the report shows that CRP may possibly be produced by aneurysmal tissue and that the level of CRP in serum is linked to the aneurysmal size.[11] This finding suggested that serum CRP might be a marker for AAA and might help to identify its condition at the earlier stages. This research was targeted to develop a highly sensitive CRP immunoassay on an antibody-attached electrode surface. Multiwalled carbon nanotubes (MWCNTs) were utilized for anti-CRP attachment on the electrode surface through the chemical linker, and then CRP interacted.

Nanomaterials have unique characteristics that make them attractive for various biomedical applications.[12–17] Specifically, carbon-based nanomaterials function as scaffolds for biomolecular immobilization on their surfaces and combine various exceptional characteristics, such as electrical, physical, chemical, and optical properties, for the transduction of signals associated with the identification of metabolites, analytes, and disease biomarkers.[18–20] Carbon nanotubes (CNTs) have recently emerged as one of the most investigated nanomaterials and offer various applications in both industrial and academic interests.[21,22] CNTs have carbon nanostructures with properly arranged carbon atoms via sp2 bonds, which provide the strongest and stiffest fibers. Functionalized nanotubes can easily cross biological barriers, such as penetrating cells and the cell membrane. This mechanism and feature of internalization show major interest in the field of intracellular biosensor applications. Apart from this, biomolecule-modified CNTs are found to be stable on the surface and arrange biomolecules correctly, which increases the interaction of the target and analyte on the sensor surface. In this work, MWCNTs were used for surface functionalization, which increases the electron transfer rate, stability, mechanical strength, and electrical conductivity.[23] Furthermore, it increases the surface area with surface physical changes and accommodates a higher number of biomolecules to interact. MWCNTs were modified on the electrode surface with a silane linker, and anti-CRP was immobilized on the MWCNTs through the aldehyde linker. On this surface, an immunoassay was conducted to quantify the level of CRP.

Highlights

- C-reactive protein (CRP) has been recognized as one of the biomarkers for identifying abdominal aortic aneurysm due to the possibility of CRP produced in vascular tissue. This research work was designed to develop an immunosensor on a multiwalled carbon nanotube-modified surface to quantify CRP. The detection limit of CRP was calculated as 200 pM.

2 | MATERIALS AND METHODS

2.1 | Reagents and biomolecules

Phosphate buffered saline (10 mM PBS; pH 7.4), CRP, and anti-human C-reactive protein (anti-CRP) were obtained from Abcam (UK). MWCNTs, APTMS (3-aminopropyl)trimethoxysilane, glutaraldehyde (GLU), and 2-aminoethyl alcohol (monoethanolamine) were obtained from Sigma–Aldrich (St Louis, Missouri, USA).

2.2 | Sensing electrode surface fabrication

A traditional wet-etching technique was used to fabricate the sensing electrode surface.[24] The interdigitated electrode (IDE) was typically designed by using AutoCAD software with the following dimensions: length, 10,000 μm; diameter, 4000 μm; two probing points with 1000 μm square and gap and finger regions (20 pairs) with a 5-μm thickness. The base silica substrate was first cleaned with Radio Corporation of America solutions (RCA1 and RCA2), and thermal oxidation was carried out at 500°C (for 1 h). On the SiO_2 layer, aluminum was coated using an aluminum coil and thermal evaporator. Afterwards, the positive photoresist was created on the aluminum surface by using a photolithography method. Furthermore, the IDE pattern was transformed by using UV light exposure. The unexposed place was removed by dipping the electrode in the photoresist developer and then baking it at 110°C (for 1 min) to remove the moist content. Finally, the unexposed aluminum layer was etched with etchant solution. The fabricated electrode was cleaned with acetone and distilled water, and further surface modification was conducted.

2.3 | Silanation process on MWCNTs

MWCNTs (0.5 g) were dispersed in 500 mL of ethanol and placed in a beaker for ultrasonication for 1 h. Then, 5 mL of 100% APTMS was added and stirred for 4 h at 70°C. Furthermore, unbound APTMS was removed by washing the MWCNTs with water followed by acetone. The final product of silanized MWCNTs (MWCNT-silane) was separated by filtration and dried under a vacuum at 100°C for 12 h.

2.4 | Construction of anti-CRP on the sensing electrode

Anti-CRP was constructed on the electrode by using a silane-aldehyde linker. The following procedures were used for the immobilization process: (i) The electrode surface was treated with KOH (1%) for 10 min; (ii) 0.5 mg/mL MWCNT-silane conjugate was added dropwise and allowed to rest for 3 h; (iii) 1% GLU was introduced and allowed to rest for 2 h; (iv) anti-CRP (250 nM) was added; and (iv) 1 M monoethanolamine was introduced and allowed to wait for 1 h. Before each process, the electrode surface was washed with PBS, and the current response was recorded.

2.5 | Immunosensor procedure for CRP detection

The CRP immunosensor was conducted on anti-CRP on the constructed surface. Initially, a higher concentration of CRP (3000 pM) was dropped on the anti-CRP-modified surface, and, then, it was incubated for 30 min to allow the CRP to interact with the antibody. After washing the surface with PBS, the current response was recorded and compared with zero CRP (only antibody). Similar experiments were conducted for all CRP concentrations (100 and 1500 pM), and the current levels were recorded. The difference for all CRP concentrations was calculated, and a linear regression graph was made to calculate the CRP limit of detection.

2.6 | Reproducibility and selectivity of CRP detection

Sensing surface reproducibility was analyzed by conducting similar experiments using five different surfaces prepared with the same batch, and the current responses were compared. The same optimal concentrations of APTMS (1%), GLU (2%), anti-CRP (250 nM), monoethanolamide (1 M), and CRP (3000 pM) were used based on the preliminary assessments. Quantification of CRP in serum samples was carried out by conducting the experiment under optimized conditions with serum-spiked CRP. CRP was spiked in human serum, and the same procedure was followed. Other biomolecular concentrations remain the same. The current responses were recorded for each CRP concentration. The changes in the current–voltage were measured by an ammeter in the optimal range of 0–2 V with intervals of 0.1 V. All experiments were carried out at room temperature and maintained under wet conditions using 10 mM PBS. Unless otherwise stated, washings were conducted between each modification or interaction step. The experiments and biomolecular interactions were carried out under wet conditions. Experiments were performed in triplicate using devices fabricated from the same batch.

3 | RESULTS AND DISCUSSION

A CRP immunosensor was developed on an MWCNT-immobilized surface to diagnose AAA (Figure 1A). Initially, the intactness of the sensing surface (Figure 1B) and MWCNTs (Figure 1C) were evaluated under a scanning electron microscope. The IDE sensing surface used in this study operates based on the dipole moment among ions during immobilization and interaction processes (Figure 2A). Anti-CRP was constructed on the surface through silane and aldehyde linkers. The MWCN increases the surface area with surface physical changes and accommodates a higher number of antibodies to interact with the target. First, the surface was hydroxylated by KOH, and then MWCNT-silane conjugation was added.[25] Here, KOH was used to enhance the silane reaction with high OH tethering. Then, GLU was used to link MWCNT-silane and anti-CRP. GLU has two aldehydes at its ends to link these amine molecules. Furthermore, to cover the free space of the aldehyde, monoethanolamine was used. Monoethanolamine helps to cover the extra space on MWCNT-silane and reduces the biofouling of CRP, which is the necessary step to reduce the signal-to-noise ratio. Finally, CRP was added to determine the interaction with its antibody. The molecular attachment on the sensing surface was also confirmed by three-dimensional (3D) nanoprofiler imaging (Figure 2B). With this surface functionalization, MWCNTs were used for the purpose of improving conductivity and increasing the amount of anti-CRP immobilization. Since the MWCNT-silane-modified surface accommodates a larger number of antibodies through the aldehyde linker, it improves the detection of

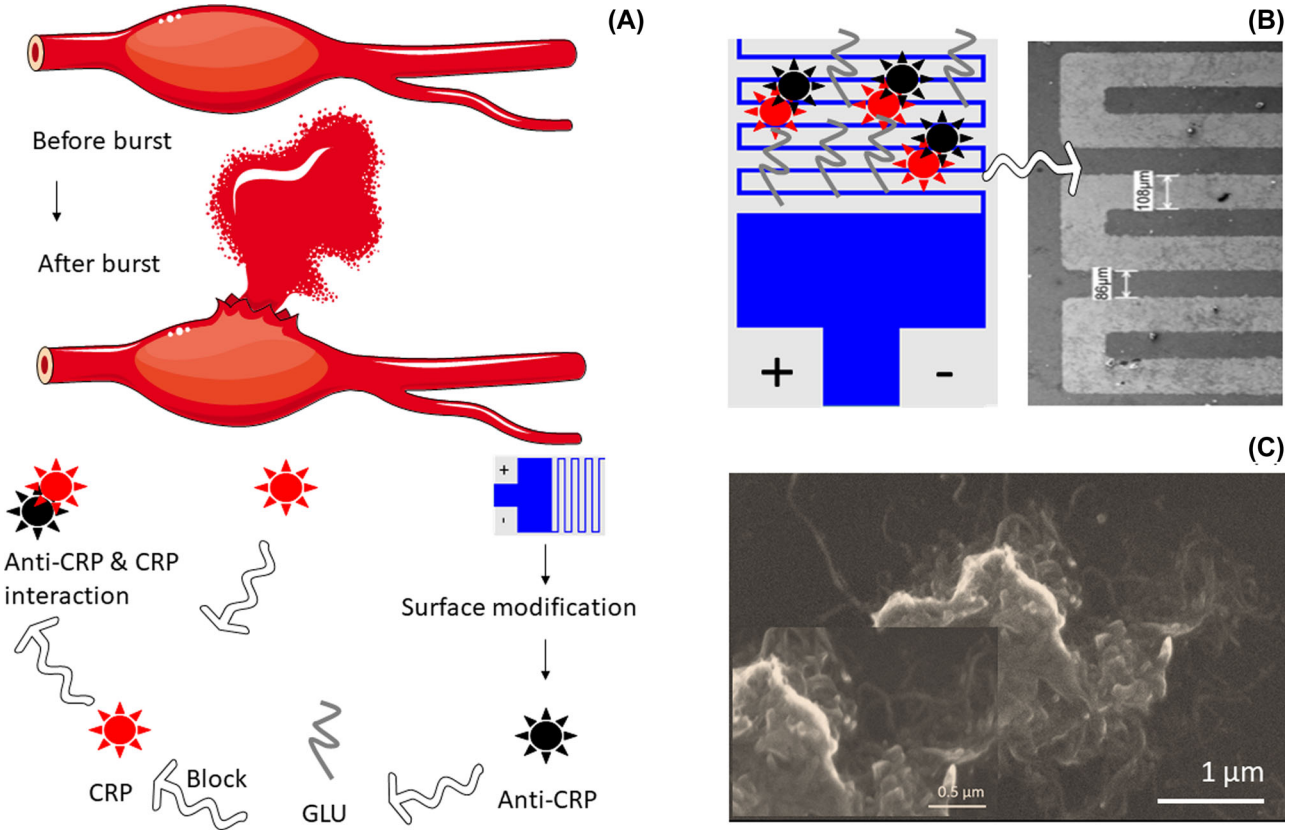

FIG 1 (A) Graphical illustration of the CRP immunosensor. Anti-CRP was constructed on the surface through silane and aldehyde linkers. Silane-modified MWCNTs were attached to the surface, and then, a GLU linker was used to immobilize anti-CRP on the MWCNT surface. Monoethanolamine was used as the blocking agent. The rupture with AAA is shown as an inset. (B) Interdigitated electrode surface with its scanning electron microscope imaging. (C) Scanning electron microscope image of MWCNTs

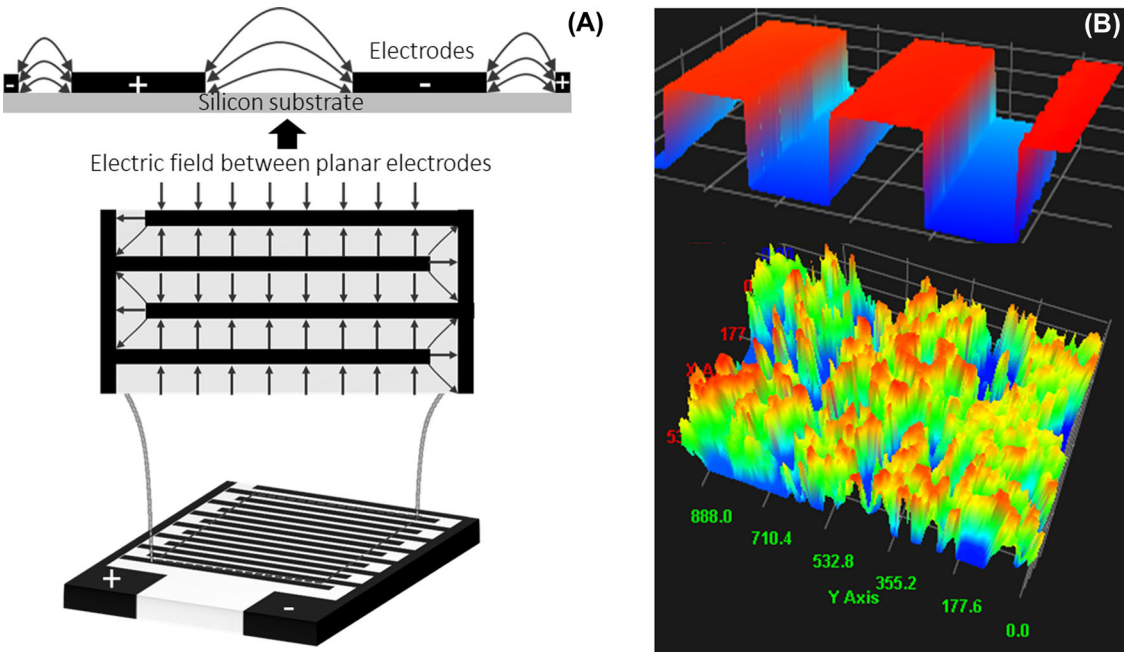

FIG 2 Surface of the interdigitated electrode. (A) Molecular mechanism and movement on the surface. (B) 3D nanoprofiler imaging before (upper image) and after (lower image) molecular immobilization

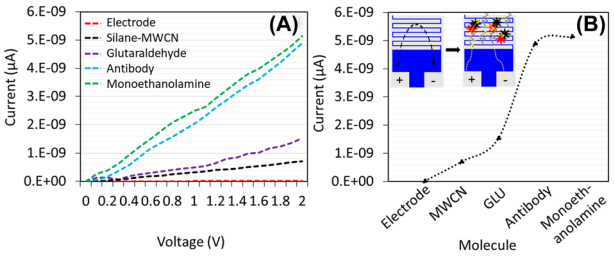

FIG 3 (A) Anti-CRP construction process. The increment of current was recorded after each step. Drastic improvement in current was noted after adding anti-CRP. (B) Current levels with the anti-CRP construction process. Anti-CRP immobilization shows the highest response to the current. The inset is a diagrammatic representation of the mechanism of the dipole moment on the sensing surface. Data were averaged from three independent experiments.

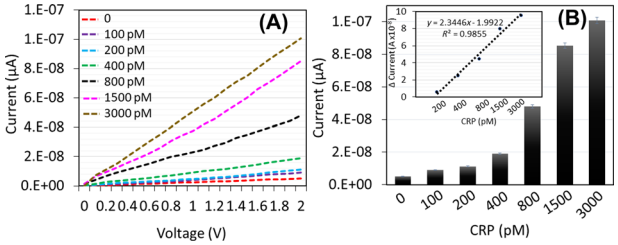

FIG 4 (A) Immunoassay for CRP identification. A CRP immunoassay was conducted on the anti-CRP constructed surface. CRP concentrations from 100 to 3000 pM were added to the antibody-constructed surface. A clear increase in the current response was recorded for all CRP concentrations. (B) The current response to CRP identification. With increasing CRP levels, the current responses also increased gradually. The current differences for all CRP concentrations binding with its antibody were placed in linear regression, and the CRP detection limit was calculated as 100 pM with an R^2 value of 0.99 (inset figure). Data were averaged from three independent experiments.

CRP. Various studies have proven that a higher and proper arrangement of the capture molecule construction on the sensor surface improves the target–analyte binding and lowers the detection limit. Due to the higher anti-CRP immobilization with MWCNTs, it was expected to improve the detection of CRP.

3.1 | Confirmation of anti-CRP construction

The anti-CRP construction process was confirmed by comparing the current responses with each immobilization step (Figure 3). As shown in Figure 3A, the surface with KOH showed a current of 1.33 E-11 A, and it changed to 5.08E-10 A after the surface was modified with silane-MWCNTs, which confirmed the surface modification with MWCNTs. Furthermore, when GLU was added, the level of the current increased to 9.79E-10 A, which showed the binding of the aldehyde with silane on the surface of the MWCNTs. When anti-CRP was further introduced, the current output displayed large changes (3.41E-09 A) and confirmed antibody attachment on MWCNTs through the silane and aldehyde linkers. On these antibody-constructed surfaces, a CRP immunoassay was employed to quantify the CRP level. In the present study, the current–voltage analysis was carried out at the lower optimal range of 0–2 V with the desired intervals (0.1 V). The desired lower range was due to the mechanism (dipole moment) occurring on the sensing surface upon biomolecular/molecular attachment and their interactions (Figure 3B; inset). The measurement with the dipole moment worked well at lower current ranges, and it became marginal when the current increased to higher levels.

3.2 | Immunoassay for CRP identification

A CRP immunoassay was conducted on the anti-CRP constructed surface. To reduce biofouling, monoethanolamine was used as a blocking agent to cover the free aldehyde before detecting CRP. Due to the anti-CRP attachment on the MWCNTs, there was a slight current response recorded after adding monoethanolamine (Figure 3B). Afterwards, CRP concentrations from 100 pM to 3 nM were dropped independently on the antibody-constructed surface, and the current responses were recorded. A 100 pM CRP solution altered the current from 6.27E-10 A to 1.37 E-09 A, which confirmed the detection of 100 pM CRP (Figure 4A). Upon further increasing the CRP concentration to 200, 400, 800, 1500, and 3000 pM, the currents were increased to 1.88 E-09, 3.5 E-09, 9.21 E-09, 1.25 E-08, and 1.52 E-08 A, respectively. When the CRP levels increased, the current responses also gradually increased (Figure 4B). The current difference for all CRP was plotted in linear regression, and the CRP detection limit was calculated to be 200 pM at an R^2 value of 0.99 (Figure 4B; inset).

3.3 | Reproducibility and selectivity of CRP detection

The reproducibility of the CRP immunosensor was confirmed by conducting the same experiments with five different surfaces fabricated from the same batch. As shown in Figure 5A, the current response was relatively the same for all biomolecular immobilizations and CRP identification. This result confirms the reproducibility of

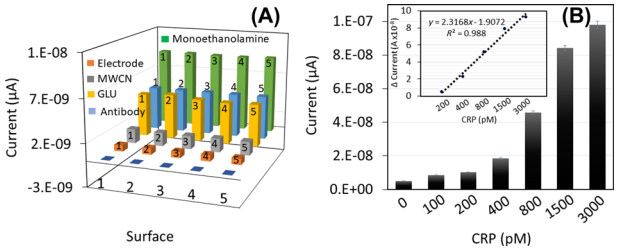

FIG 5 (A) Reproducibility of the CRP immunosensor. Similar surface functionalization was used with five surfaces for CRP identification, and the current response was relatively the same for all experiments. (B) A CRP selectivity experiment was carried out with CRP-spiked human serum. CRP was spiked in optimized serum dilution (1:100), and the required volume on the anti-CRP constructed surface was dropped. Serum dilution did not affect CRP detection, which confirms the selective identification of CRP. Data were averaged from three independent experiments.

the immunosensor for the identification of CRP. The selectivity of CRP was determined by an experiment with CRP-spiked human serum. For optimization, different dilutions (1:10, 1:100, and 1:1000) of serum were initially compared with CRP-spiked buffer solution to reveal biofouling. Based on the optimization study, CRP was spiked in human serum at 1:100 and dropped on the anti-CRP constructed surface. This preliminary assessment with a serum dilution of 1:100 displayed a negligible background signal with high nonfouling. This will enhance the sensitivity and specificity of the biosensor demonstrated. As shown in Figure 5B, the serum did not affect the detection of CRP. With increases in CRP, the current also gradually increased, which confirmed the selective identification of CRP. Furthermore, the recovery percentages were calculated for the concentrations (100, 200, 400, 800, 1500, and 3000 pM) used and were 92.2%, 93.5%, 95.8%, 97.13%, 97.4%, and 98.8%, respectively. The obtained results indicate the minor interference of proteins from serum for the interaction of CRP and anti-CRP. The serum has two major interfering proteins, namely, albumin, and globulin, at levels of 3.5–5.0 and 2.6–3.5 g/dL, respectively, which might play a major role. Compared to other sensing systems, the current sensor provides a high surface with modification by MWCNTs and facilitates spatial arrangements for biomolecular/molecular assembly.

4 | CONCLUSION

The AAA is a swollen and enlarged area of the abdominal aorta, which is a life-threatening issue when it ruptures and breaks. Quantifying CRP in serum biomarkers helps to identify AAA and the associated conditions. CRP was recognized as a suitable biomarker for AAA, and an elevated level of AAA was found in a patient with a ruptured aneurysm. A CRP immunoassay was conducted on a MWCNT-modified surface. Silane-modified MWCNTs were attached to the surface, and, then, a GLU linker was used to attach the anti-CRP to the MWCNT surface. On this surface, the CRP detection limit reached 100 pM. Further reproducibility experiments were confirmed with five different chips prepared from the same batch, and similar identification of CRP on antibody-modified surfaces was observed. Then, the selectivity experiment in 1:100 diluted serum-spiked CRP confirmed the selective identification of CRP. This immunosensor identifies CRP at a lower level and can help to diagnose AAA.

ORCID

Subash C.B. Gopinath https://orcid.org/0000-0002-8347-4687
Weichao Zhao https://orcid.org/0000-0003-0560-0569

REFERENCES

1. Hong X, Hong X, Zhao H, Chen C, Gopinath Subash CB, Lim D, et al. Improved immunoassay for insulin-like growth factor 1 detection by aminated silica nanoparticle in ELISA. Process Biochem. 2020;91:282–287.
2. Springer F, Schlierf R, Pfeffer JG, Mahnken AH, Schnakenberg U, Schmitz-Rode T. Detecting endoleaks after endovascular AAA repair with a minimally invasive, implantable, telemetric pressure sensor: an in vitro study. Eur Radiol. 2007;17:2589–97.
3. Sweeting MJ, Patel R, Powell JT, Greenhalgh RM. Endovascular repair of abdominal aortic aneurysm in patients physically ineligible for open repair. N Engl J Med. 2010;362:1872-80.
4. Takagi H, Manabe H, Kawai N, Goto S, Umemoto T. Circulating matrix metalloproteinase-9 concentrations and abdominal aortic aneurysm presence: a meta-analysis. Interact Cardiovasc Thorac Surg. 2009;9:437–440.
5. Yan G, Li Q, Hong X, Gopinath SCB, Anbu P, Li C, et al. An iron oxide nanoworm hybrid on an interdigitated microelectrode silica surface to detect abdominal aortic aneurysms. Microchim Acta. 2021;188:185.
6. Montano N, D'Alessandris QG, Izzo A, Fernandez E, Pallini R. Biomarkers for glioblastoma multiforme: status quo. J Clin Transl Res. 2016;2:3–10.
7. Mcgill MR, Jaeschke H. Biomarkers of mitotoxicity after acute liver injury: further insights into the interpretation of glutamate dehydrogenase. J. Clin Transl Res. 2021;7:61–65.
8. Liu Q, Ding J, Liu Y, Jiang Z, Li Lin, Xiao XinBing, et al. The novel biomarkers in the diagnosis of prostate cancer. Cancer plus. 2019;1:8–16.
9. Yang Z, Zhang N, Shen Z, Bai S, Shi M. Markers for early diagnosis and postoperative recurrence monitoring of bladder cancer. Cancer plus. 2020;2:43–52.
10. Vainas T, Lubbers T, Stassen FRM, Herngreen SB, van Dieijen-Visser MP, Bruggeman CA, et al. Serum C-reactive protein level is associated with abdominal aortic aneurysm size and may be produced by aneurysmal tissue. Circulation. 2003;107:1103–5.
11. Badger SA, Soong CV, O' Donnell ME, Mercer C, Young IS, Hughes AE. C-reactive protein (CRP) elevation in patients with

abdominal aortic aneurysm is independent of the most important CRP genetic polymorphism. J Vasc Surg. 2009;49:178–84.
12. Hou Y, Wang W, Bártolo P. Investigating the effect of carbon nanomaterials reinforcing poly(ε-caprolactone) printed scaffolds for bone repair applications. Int J Bioprinting. 2020;6:1–9.
13. Shuai C, Li Y, Yang W, Yu L, Yang Y, Peng S, et al. Graphene oxide induces ester bonds hydrolysis of poly-l-lactic acid scaffold to accelerate degradation. Int J Bioprinting. 2020;6:91–104.
14. Rueda-Gensini L, Serna JA, Cifuentes J, Cruz JC, Muñoz-Camargo C. Graphene oxide-embedded extracellular matrix-derived hydrogel as a multiresponsive platform for 3D bioprinting applications. Int J Bioprinting. 2021;7:1–16.
15. Chen S, Jang TS, Pan HM, Jung HDO, et al. 3D freeform printing of nanocomposite hydrogels through in situ precipitation in reactive Viscous fluid. Int J Bioprinting. 2020;6:1–21.
16. Carrasco-esteban E, Domínguez-rullán JA, Barrionuevo-castillo P, Pelari-mici L, López-campos F. Current role of nanoparticles in the treatment of lung cancer. J Clin Transl Res. 2021;7:140–55.
17. Zhang Y, Attarilar S, Wang L, Lu W, Yang J, Fu Y. A review on design and mechanical properties of additively manufactured NiTi implants for orthopedic applications. Int J Bioprinting. 2021;7:15–42.
18. Yao J, Li S, Zhang L, Yang Y, Gopinath SCB, Lakshmipriya T, et al. Aptamer-antibody dual probes on single-walled carbon nanotube bridged dielectrode: comparative analysis on human blood clotting factor. Int J Biol Macromol. 2020;151:1133–8.
19. Ong CC, Siva Sangu S, Illias NM, Chandra Bose Gopinath S, Saheed MSM. Iron nanoflorets on 3D-graphene-nickel: a 'dandelion' nanostructure for selective deoxynivalenol detection. Biosens Bioelectron. 2020;154:112088.
20. Koch L, Brandt O, Deiwick A, Chichkov B. Laser-assisted bioprinting at different wavelengths and pulse durations with a metal dynamic release layer: a parametric study. Int J Bioprinting. 2017;3:42–53.
21. Taghdisi SM, Emrani SS, Tabrizian K, Ramezani M, Abnous K, Emrani AS. Ultrasensitive detection of lead(II) based on fluorescent aptamer-functionalized carbon nanotubes. Environ Toxicol Pharmacol. 2014;37:1236–1242.
22. Liang T, Qu Q, Chang Y, Gopinath SCB, Liu XT. Diagnosing ovarian cancer by identifying SCC-antigen on a multiwalled carbon nanotube-modified dielectrode sensor. Biotechnol Appl Biochem. 2019;66:939–944.
23. Oliveira TMBF, Fátima Barroso M, Morais S, De Lima-Neto P, Oliveira MB, Delerue-Matos C. Biosensor based on multiwalled carbon nanotubes paste electrode modified with laccase for pirimicarb pesticide quantification. Talanta. 2013;106:137–143.
24. Liang T, Qu Q, Chang Y, Gopinath SCB, Liu XT. Diagnosing ovarian cancer by identifying SCC-antigen on a multiwalled carbon nanotube-modified dielectrode sensor. Biotechnol Appl Biochem, 2019;66:939–944.
25. Dixit CK, Vashist SK, O'neill FT, O'reilly B, MacCraith BD, O'Kennedy R. Development of a high sensitivity rapid sandwich ELISA procedure and its comparison with the conventional approach. Anal Chem. 2010;82:7049–7052.

How to cite this article: Zhao X, Gopinath SCB, Zhao W. Immuno-probed multiwalled carbon nanotube surface for abdominal aortic aneurysm biomarker analysis. Biotechnology and Applied Biochemistry. 2022;1–7.
https://doi.org/10.1002/bab.2372